Published OnlineFirst September 16, 2019; DOI: 10.1158/2326-6066.CIR-19-0107

Cancer Immunology Miniatures

Cancer Immunology Research

Direct Detection and Quantification of Neoantigens

Qing Wang[1,2], Jacqueline Douglass[1,2], Michael S. Hwang[1,2], Emily Han-Chung Hsiue[1,2], Brian J. Mog[1,2], Ming Zhang[1,2], Nickolas Papadopoulos[1,2], Kenneth W. Kinzler[1,2], Shibin Zhou[1,2], and Bert Vogelstein[1,2]

Abstract

Many immunotherapeutic approaches under development rely on T-cell recognition of cancer-derived peptides bound to human leukocyte antigen molecules on the cell surface. Direct experimental demonstration that such peptides are processed and bound is currently challenging. Here, we describe a method that meets this challenge. The method entailed an optimized immunoprecipitation protocol coupled with two-dimensional chromatography and mass spectrometry. The ability to detect and quantify minute amounts of predefined antigens should be useful both for basic research in tumor immunology and for the development of rationally designed cancer vaccines.

Introduction

Proteins encoded by mutant genes in cancers can be processed and presented by human leukocyte antigen (HLA) molecules on a cell surface. In some cases, this processing can result in presentation of peptides containing "Mutation-Associated Neoantigens" (MANA), which can be recognized by T cells (1). The effectiveness of immune checkpoint inhibitors, such as PD-1 antibodies, is dependent on recognition of such MANAs (2). Many other types of immunotherapies are currently being developed to exploit MANAs with either immune modulation or vaccines composed of the MANAs themselves (2–4). The durable responses achieved with immunotherapies against cancer are often remarkable (5, 6).

One of the rate-limiting steps in understanding and developing MANA-based therapies is the identification of HLA-presented MANAs. Although genetic mutations within cancer cells can now be routinely identified through exome-wide sequencing, the determination of which mutations result in altered peptides that are properly processed and actually presented on the patient's HLA molecules on the surface of cells remains difficult (7). As a result, such determinations are rarely performed experimentally (4, 8), but rather rely on predictions of binding affinity performed *in silico* (4). These *in silico* predictions have proved to be very helpful but are not particularly sensitive or specific (9). Alternatively, MANAs can be determined experimentally by culturing tumor cells or antigen-presenting cells (peptide-pulsed or transfected with antigen-encoding plasmids) with autologous T cells to expand MANA-reactive T cells, with validation provided by tetramer staining or peptide-pulsing assays (10, 11). However, these experimental methods require the presence of endogenous T-cell clones recognizing the putative MANAs and are technically difficult due to the low abundance of most MANA-reactive T-cell clones relative to all T-cell clonotypes. Thus, facile experimental techniques for confirming these predictions or for testing potentially important MANAs that do not score in the predictive algorithms are needed and would likely improve the odds of successful immunotherapy (7).

The most direct way to test whether an individual MANA is presented on the surface of a cell is through mass spectrometry (MS; ref. 12). The mutant genes and corresponding HLAs of interest can be transfected into cells, and antibodies reactive against HLA molecules can be used to immunoprecipitate the HLA–peptide complexes on the cell surface. Mass spectrometry can then, in theory, be used to determine whether the MANA is present within the immunoprecipitate but, in practice, any individual MANA represents only a tiny fraction of the immunoprecipitated complexes, and their detection has proved challenging (12, 13). Thus, commonly used MS-based techniques for detecting abundant peptides are not applicable (12). To our knowledge, the only published MS-based technique for targeted detecting presented peptides required 2.0 to 6.7 billion cells and the efficiency of recovering MANA-related peptides was only 1% to 3% (14). To overcome this obstacle, we have developed a technique, called Mutation-Associated Neoantigen Selected Reaction Monitoring (MANA-SRM), that permits the direct detection and quantification of HLA-binding MANAs.

Materials and Methods

Materials

Cell lines. COS-7, CFPAC-1, Hs578.T, HL-60, HH, SW948, RD, Hs940.T, and RPMI-6666 cells were obtained from the ATCC between 2014 and 2018. COS-7, CFPAC-1, and SW948 were

[1]Ludwig Center, Johns Hopkins Kimmel Cancer Center, Baltimore, Maryland. [2]Howard Hughes Medical Institute, Johns Hopkins Kimmel Cancer Center, Baltimore, Maryland.

Note: Supplementary data for this article are available at Cancer Immunology Research Online (http://cancerimmunolres.aacrjournals.org/).

Q. Wang and J. Douglass contributed equally to this article.

Corresponding Authors: Bert Vogelstein, Johns Hopkins Kimmel Cancer Center, CRB I, Room 589, 1650 Orleans Street, Baltimore, MD 21231. Phone: 410-955-8878; E-mail: bertvog@gmail.com; Qing Wang, wangqingok@gmail.com; and Shibin Zhou, sbzhou@jhmi.edu

Cancer Immunol Res 2019;7:1748–54

doi: 10.1158/2326-6066.CIR-19-0107

Published OnlineFirst September 16, 2019; DOI: 10.1158/2326-6066.CIR-19-0107

cultured in McCoy's 5A Media (Thermo Fisher Scientific) with 10% FBS (HyClone) and 1% penicillin–streptomycin (Thermo Fisher Scientific). Hs578.T, Hs940.T, and RD were cultured in Dulbecco's Modified Eagle's Media (Thermo Fisher Scientific) with 10% FBS (HyClone) and 1% penicillin–streptomycin (Thermo Fisher Scientific). HL-60 was cultured in Iscove's Modified Dulbecco's Medium (ATCC) with 20% FBS and 1% penicillin–streptomycin. HH was cultured in RPMI-1640 (ATCC) with 10% FBS and 1% penicillin–streptomycin. RPMI-6666 was cultured in RPMI-1640 (ATCC) with 20% FBS and 1% penicillin–streptomycin. Upon receipt of each cell line, the line was expanded, and stock vials were frozen. Each cell line was cultured for no longer than 6 months before thawing a new vial from the original stock. Cell lines were not reauthenticated but were routinely tested for *Mycoplasma*.

Antibodies. Purified anti-human HLA-A, B, C antibody (clone W6/32) was purchased from Bio X Cell. Anti–HLA-DR antibody (L243) was purchased from Abcam.

Plasmids. Plasmids encoding KRAS (wild-type, G12C, G12D, G13D, Q61H, Q61L, and Q61R), IDH2 (wild-type and R140Q mutant), and HLA class I alleles (A1, A2, A3, B7) followed by a T2A sequence and the *GFP* gene were synthesized and cloned into pcDNA3.1 by GeneArt (Thermo Fisher Scientific). An exemplary plasmid map showing a gene of interest (HLA or Oncogene) followed by the T2A and GFP as well as the sequence inserts used is provided (Supplementary Fig. S1; Supplementary Table S1). All other reagents were purchased from Sigma-Aldrich unless otherwise indicated.

Preparation of solutions. *Lysis buffers.* Lysis buffer I (10 mL) contained 6.87 mL RIPA buffer (68.7 µL Nonidet P-40, 687 µL 10% wt/vol sodium deoxycholate, 68.7 µL 10% wt/vol SDS; Invitrogen), 206.1 µL 5 M NaCl, 68.7 µL 1 M sodium phosphate (pH 7.2), 1 mL water, one Complete EDTA-free Protease Inhibitor Mixture tablet (Roche), 1 mL 0.5 M NaF, 10 µL 80 mmol/L b-glycerophosphate, 1 mL 20 mmol/L Na pyrophosphate, 10 µL 300 mmol/L Na orthovanadate, 10 µL 1 M DTT, and 100 µL 100 mmol/L PMSF. Lysis buffer II (10 mL) was a buffer reported to extract and enrich membrane proteins, and it was prepared in PBS containing 0.25% sodium deoxycholate, 0.2 mmol/L iodoacetamide, 1 mmol/L EDTA, 1:200 Protease Inhibitors Cocktail (Sigma-Aldrich), 1 mmol/L PMSF, and 1% octyl-β-D glucopyranoside (Sigma-Aldrich; ref. 15). Lysis buffer III (10 mL) was a buffer reported to specifically enrich HLA-binding peptides, and it was composed of 0.5% IGEPAL 630, 150 mmol/L NaCl, and 50 mmol/L Tris (pH 8.0; ref. 16).

Modified RIPA buffer. Modified RIPA buffer (10 mL) contained 300 µL 5 M NaCl, 500 µL 1 M Tris (pH 7.4), 100 µL Nonidet P-40, 250 µL 10% (wt/vol) sodium deoxycholate, 20 µL 0.5 M EDTA, and 8.83 mL water.

Immunoprecipitation buffers. Immunoprecipitation (IP) system I is composed of lysis buffer I and modified RIPA buffer; IP systems II and III are composed of lysis buffers II and III, respectively, as described (15, 16).

Antibody conjugation reaction buffer. Antibody conjugation reaction buffer (ACRB, 0.2 M triethanolamine [pH 8.2] and 25 mmol/L dimethyl pimelimidate dihydrochloride) was prepared fresh before each use.

Neoantigen elution buffer. Neoantigen elution buffer (NEB) contained 50 mmol/L ammonium bicarbonate and 50% acetic acid (pH 2.0).

bRPLC solvents. bRPLC solvent A contained 15 mmol/L triethylammonium bicarbonate; bRPLC solvent B contained 90% (vol/vol) acetonitrile, 15 mmol/L triethylammonium bicarbonate.

Mass spectrometry solvents. Solvent A contained 3% (vol/vol) acetonitrile, 0.1% formic acid; solvent B contained 90% (vol/vol) acetonitrile, 0.1% formic acid.

Cell transfection

COS-7 cells seeded into 24.5×24.5 cm^2 plates were transfected with plasmids containing the genes indicated above at 95% confluency using Lipofectamine 3000 Reagent (Thermo Fisher Scientific). For each plate, 125 µg of plasmid (50 µg of HLA plasmid and 75 µg of mutant or wild-type protein plasmid) was mixed with 200 µL of Lipofectamine P3000 in 6 mL of Opti-MEM (Thermo Fisher Scientific). In a separate tube, 200 µL of Lipofectamine 3000 Reagent was mixed with 6 mL of Opti-MEM. The contents of the two tubes were mixed and allowed to complex for 10 minutes. Medium bathing cells were removed, and 50 mL of fresh complete medium was added followed by the Lipofectamine–DNA mixture. Cells were harvested 48 to 72 hours after transfection. The transfection efficiencies of COS-7 cells were measured to be 93.5% ± 4.9%, in multiple assays as assessed by GFP$^+$ fraction on flow cytometry (BD LSRII). Representative data for assessing transfection efficiencies are displayed in Supplementary Fig. S2.

Generation of the *KRAS* G12D-knock-in cell line

The CFPAC-1 G12D knock-in cell line was generated by coelectroporation of a Cas9 ribonucleoprotein (RNP) obtained from Integrated DNA Technologies, Inc. (IDT) targeting the *KRAS* locus with a single-stranded DNA oligo repair template encoding the *KRAS* G12D mutation. The G12D repair template was designed with asymmetric homology arms of 72 and 40 base pairs and an altered PAM site to increase the rate of homology directed repair (17). A coselection strategy simultaneously targeting the ATP1A1 locus with a Cas9 RNP and repair template was used to enrich for edited cells (18). Alt-R CRISPR Cas9 crRNAs (Integrated DNA Technologies) targeting *KRAS* exon 2 (AATGACTGAATATAAACTTG) and ATPA1 (GTTCCTCTTCTGTAGCAGCT) were duplexed individually with Alt-R CRISPR-Cas9 tracrRNA (IDT) for 5 minutes at 95°C. Duplexed RNA was cooled to room temperature before mixing at a 1.1:1 molar ratio with Cas9 Nuclease (IDT) for 10 minutes at room temperature. The *KRAS* G12D and ATP1A1 repair templates were ordered as Ultramer DNA oligonucleotides and resuspended at a concentration of 100 µmol/L in TE buffer (Thermo Fisher Scientific). To electroporate, the following components were combined in a 20 µL reaction volume in Opti-MEM (Thermo Fisher Scientific): *KRAS* RNP (1 µmol/L), ATP1A1 RNP (1 µmol/l), *KRAS* G12D repair template (2.5 µmol/l), ATP1A1 repair template (2.5 µmol/L), and CFPAC-1 cells (20e6 cells/mL). The electroporation was performed in a 0.1-cm cuvette (Bio-Rad Laboratories) using an ECM 2001 (BTX). Electroporated cells were allowed to recover in culture in their

Published OnlineFirst September 16, 2019; DOI: 10.1158/2326-6066.CIR-19-0107

normal growth medium for 3 days before selection with 0.5 μmol/L ouabain (Sigma-Aldrich) for 10 days. Selected cells were plated by limiting dilution in their normal growth medium and incubated for 3 weeks. Individual clones were screened by isolating genomic DNA using the Quick-DNA 96 Kit (Zymo Research), PCR amplifying a 1-kb window surrounding the edit site 1 to 10 ng of template DNA, and Sanger sequencing to identify and confirm the introduced G12D mutation (Supplementary Fig. S3). *KRAS* G12D repair template sequence is 5′-ATTGTTGGATCATATTC-GTCCACAAAATGATTCTGAATTAGCTGTATCGTCAAGGCACTC-TTGCCTACGCCATCAGCTCCAACTACGACAAGTTTATATTCAG-TCATTTTCAGCAGGCCTTATAATA-3′.

Cell lysis and protein quantification

Cultured cells (transfected or untransfected) were grown to near confluency in 24.5 × 24.5 cm^2 plates. Cultured cells were washed with PBS two times, followed by another wash with prechilled PBS at 4°C containing 1× cOmplete Protease Inhibitor (Sigma-Aldrich). Cells were scraped directly and collected in a falcon tube. The tube was centrifuged at 1,000 × *g* for 5 minutes, and the supernatant was removed. Cell pellets were snap frozen in liquid nitrogen and stored at −80°C for future experiments.

Lysis buffer was added to the cell pellets at a ratio of 50 million cells per 1 mL lysis buffer. Cells were lysed by incubation in lysis buffer for 30 minutes on ice, with vortexing every 10 minutes. The lysates were clarified by centrifugation at 12,000 × *g* for 30 minutes at 4°C. Lysates were stored at –80°C at a concentration of 50 mg of total protein per tube. A bicinchoninic acid (BCA) assay kit (Thermo-Scientific) was used to quantify protein concentrations on a BioTek Synergy H1 plate reader (BioTek).

Immobilization of antibody on magnetic beads

A purified human HLA-A, B, C antibody (clone W6/32; 1 mg) was added to 5 mL Protein G Dynal Magnetic Beads (purchased from Thermo Fisher Scientific at 30 mg/mL, without washing), and the antibody was allowed to bind to the beads on a rotator at 30 rpm at room temperature for 2 hours. The antibody-bound beads were then washed with 5-mL ACRB and collected using a DynaMag-50 magnet (Thermo Fisher Scientific). The antibody was covalently cross-linked to the protein G on the beads by incubation in 5-mL ACRB on a rotator at room temperature for 30 minutes. The beads were washed twice with 5-mL 50 mmol/L Tris-HCl (pH 7.5), resuspended in 5-mL 50 mmol/L Tris-HCl (pH 7.5), and rotated at 30 rpm at room temperature for 15 minutes. The cross-linking reaction was quenched by incubating the beads with 50 mmol/L Tris-HCl. The beads were resuspended in 3 mL 50 mmol/L Tris-HCl (pH 7.5), and 2 mL glycerol was added before the beads were stored at –20°C. The HLA-DR antibody (clone L243) was used to prepare conjugated beads for enriching MHC class II molecules following the same procedure indicated above.

IP of HLA molecules

Cell lysates containing 50 mg of total protein were thawed on ice and diluted with four volumes of modified RIPA buffer. Antibody-conjugated Dynal beads (5 mL) were added, and the suspension incubated at 4°C overnight (minimum of 12 hours). The beads were collected on a DynaMag-50 magnet (Thermo Fisher Scientific) and were washed three times with freshly prepared modified RIPA buffer. The HLA proteins and the HLA-binding peptides (including neoantigenic peptides) were eluted by vortexing the beads at 650 rpm in 5-mL NEB buffer for 10 minutes at room temperature. The beads were collected using a DynaMag-50 magnet (Thermo Fisher Scientific) and the supernatant was transferred to an Amicon Ultra Centrifugal Filter with a 3-kDa molecular weight cutoff (Millipore-Sigma). The filter was centrifuged at 4,000 × *g* for 30 minutes at 25°C, and the filtrate was collected and snap frozen using liquid nitrogen and lyophilized.

MANA-SRM sample group establishment

Lyophilized neoantigenic peptides were reconstituted in bRPLC solvent A, and 3% acetonitrile was added to the reconstituted sample to aid in the resolubilization of the peptides. An HPLC fractionation was performed to separate the neoantigenic peptides into 96 fractions based on each peptide's hydrophobicity in a weak basic environment (pH = 8.2). The bRPLC solvents were used for this HPLC separation performed as previously described (19). Neoantigenic peptides were then organized into 32 groups comprising three sequential fractions each, according to the MANA-SRM fraction group scheme as previously described (19). All MANA-SRM fractions of neoantigenic peptides were dried in a Speed-Vac at 35°C with vacuum pressure below 5 mbar.

Dual reduction

Eluted and lyophilized neoantigenic peptides were first reconstituted in bRPLC solvent A with 3% acetonitrile to aid the resolubilization. 200 mmol/L triethylammonium bicarbonate was added to neutralize samples and adjust the pH to ∼8. DL-dithiothreitol (DTT) was then added at 10 mmol/L to the sample followed by an incubation at 60°C for 15 minutes. After the bRPLC fractionation, each fraction group was dried and could be stored at –80°C until analysis. Each sample was reconstituted in 39-μL mass spectrometry solvent A without formic acid. The dissolved peptide sample was reduced again by tris(2-carboxyethyl)phosphine (TCEP) at 10 mmol/L at low pH (pH = 3) followed by an incubation at 60°C for 15 minutes. The reduced samples were ready for MANA-SRM mass spectrometry assays as previously described (19).

Hydrophilic interaction liquid chromatography treatment of peptides

Peptides were purified through a GlycoWorks hydrophilic interaction liquid chromatography (HILIC) cartridge purchased from Waters. The samples were dried in a Speed-Vac at 35°C with vacuum pressure below 5 mbar.

SRM method development and assay

Thirty-three heavy isotope-labeled neoantigenic peptides flanking gene mutation hotspots on cancer driver genes (including *Kras, EGFR, TP53, CTNNB1*, and *IDH2*) were predicted by NetMHC 4.0 (20) and subsequently synthesized as AQUA Peptides by Sigma-Aldrich (Supplementary Table S2). Optimization of collision energies and fractionation were performed as previously described (19). A list of the SRM transitions and fraction group IDs for all 33 peptides is shown in Supplementary Table S2. All transition parameters were manually examined and curated to exclude ions with excessive noise due to coelution with impurities. Copy number of each detectable neoantigenic peptide was calculated using heavy isotope-labeled peptides as previously described (21).

Published OnlineFirst September 16, 2019; DOI: 10.1158/2326-6066.CIR-19-0107

Data deposition

The data reported in this article have been deposited via ProteomeXchange (identifier PASS01266).

Results

MANA-SRM entailed two steps, an antibody-based neoantigen enrichment and a multidimensional chromatography-based MS assay (Fig. 1; Supplementary Table S2 and Materials and Methods). For the IP step, we first explored various ways of cross-linking anti-HLA antibodies on beads. Such cross-linking prevented coelution of the antibodies with peptides, which otherwise would have caused a major ion suppression because the amount of antibody was enormous relative to the amount of any individual peptide evaluated. After comparing different types and concentrations of cross-linkers, we found that 25 mmol/L dimethyl pimelimidate dihydrochloride (DMP) maintained the antigen-binding capability of the anti-HLA antibody as well as its firm attachment to protein G magnetic beads (Supplementary Fig. S4A). We then compared various cell lysis and IP protocols to identify one with an optimum yield of HLA molecules after binding to the anti-HLA antibody-bound beads (Supplementary Fig. S4B). Finally, we tested various elution buffers at numerous concentrations and found that 20% acetic acid in 50 mmol/L ammonium bicarbonate produced the highest HLA yield compatible with minimal release of antibody from the beads (Supplementary Fig. S4C).

Following elution, the peptides were purified from the HLA molecules by a simple filtration through a cellulose membrane. The peptides were then processed through two chromatographic steps. The first separated the peptides into 32 fractions based on hydrophobicity in a weak basic environment (pH = 8.2). The fraction containing each MANA of interest was identified using a synthetic heavy isotope-labeled peptide identical in sequence to the MANA. This fraction was subjected to a second, reverse phase HPLC-based separation linked directly to the mass spectrometer. Selective reaction monitoring was used for the specific detection of each MANA after identifying the optimum collision energies, transitions, and other parameters required for SRM-based analyses.

Two further modifications of this overall approach were required for the efficient detection of MANAs. First, we noticed contaminants with characteristic 44-Da peak intervals in MS2 scans, which we interpreted to represent polyethylene glycol (PEG) derivatives (Supplementary Fig. S5). PEG-based detergents (e.g., NP-40) are commonly used in cell lysis and IP buffers (22). We found that these contaminants could be removed with a HILIC matrix (Supplementary Fig. S6). Second, many potential MANAs contain unstable amino acids such as cysteine or methionine. Peptides containing such residues are typically not chosen for targeted analysis by MS (23). Such exclusion is generally not detrimental when analyzing proteins in general, because there are usually numerous other peptides from the same protein that do not contain unstable amino acids and are preferable for targeted evaluation. However, in the case of MANAs, there is only one peptide of interest to be evaluated and no other peptides from the protein can substitute for it. We found that such unstable peptides could be stabilized through a dual-reduction strategy (Materials and Methods). The peptides were reduced first with DTT at pH 8.2 prior to bRPLC fractionation and subsequently reduced at low pH before the second chromatographic step. This dual-reduction approach improved the signals obtained from Cys- or Met-containing peptides by more than 300-fold (Supplementary Table S3).

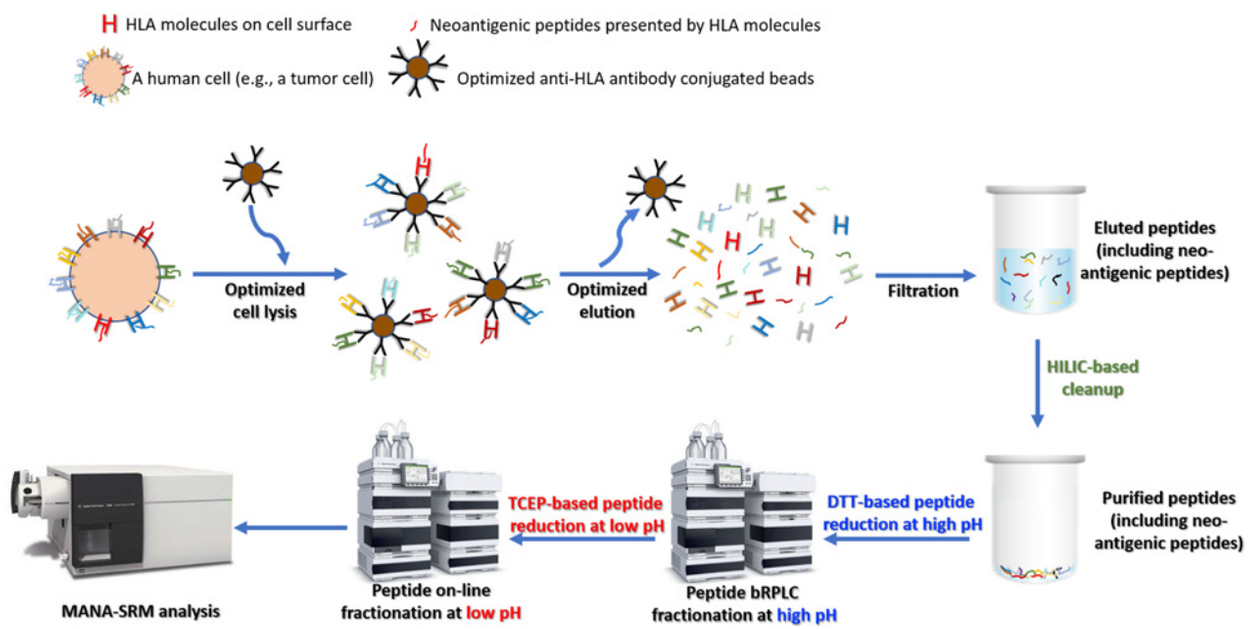

Figure 1.

Schematic of the MANA-SRM pipeline. Cells were lysed, and HLA-binding peptides were enriched through IP with an antibody targeting HLA molecules. HLA molecules together with their presented peptides were eluted and dissociated. The eluate containing the neoantigenic peptide was filtered where only short peptides (MW < 3 kDa) were allowed to pass through. The filtered peptide sample was lyophilized and made ready for MANA-SRM analysis with additional improvements through HILIC-based cleanup and the dual reduction (D-Red) strategy (see details in Materials and Methods).

Published OnlineFirst September 16, 2019; DOI: 10.1158/2326-6066.CIR-19-0107

We then tested the quantitative performance of MANA-SRM, including its linearity and range of detection. For this purpose, various amounts (0.2–2 μg) of HLA–peptide complexes with different HLA types were spiked into a cell lysate prepared from 35 million SW480 cells prior to IP. In all cases, over 95% of the spiked-in HLA–peptide complexes were recovered, as assessed by subsequent Western blot assays (Supplementary Fig. S4D). The amount of 2 μg for HLA–peptide complexes is equivalent to 800,000 HLA molecules per cell, which is far greater than the amount expressed in cells *in vivo* or in the cells used in the experiments reported below. We concluded that this IP protocol should be able to recover nearly all the HLA–peptide complexes present.

We next tested 33 potential MANA-related peptides covering residues that are frequently mutated in human cancers, each of which was spiked into the eluted antigen solutions following IP from SW480 cell lysates. The purpose of these experiments was to determine whether the peptides could be detected in the context of IP eluates from cell lysates using the MS component of MANA-SRM rather than to test the efficiency of the IP component. We found that all 33 peptides could be detected, and that the signal strength of each of the peptides was at least 70% of the signal strength of the same peptides measured in the absence of IP eluates (Supplementary Fig. S7). This excellent performance was dependent on several aspects of MANA-SRM. For example, in the absence of the HILIC purification step, 16 of the 33 peptides had weak signals (<10% of the expected values; Supplementary Fig. S6), and in the absence of dual reduction, 11 of the 33 peptides were undetectable (Supplementary Table S3).

To test the efficiency of the entire MANA-SRM process, various amounts of HLA–peptide complexes were spiked into an SW480 cell lysate. Seven different complexes were tested, and an average of 74% of the peptides was recovered as assessed by MS. Additionally, we demonstrated that the same method could be used to quantify peptides presented by HLA class II molecules (see Materials and Methods). In similar spike-in experiments, we recovered 71% of CLIP DR1*0101 complexes loaded with PVSKMRMATPLLMQA and 73% of HIV Integrase DR1*0101 complexes loaded with SGYIEAEVIPAETGQET (Supplementary Table S4).

Based on the success of these validating experiments, we sought to determine whether MANA-related peptides of interest were actually processed and presented on the surface of cells expressing particular HLA alleles. In these experiments, monkey COS-7 cells were transfected with HLA genes as well as oncogenes predicted to generate MANAs that could bind to the HLA gene products. The MANAs tested included those derived from several different common mutant forms of KRAS, as well as one from IDH2. In each case, synthetic heavy isotope-labeled peptides were generated that corresponded to the 9- or 10-amino acid peptides predicted to bind to particular HLA alleles.

We found that some of the predicted peptides were processed and presented, whereas others were not (Table 1). We were also able to quantify the number of copies of the peptides bound to HLA on the surfaces of these cells. For example, 196 copies of a KRAS G12D MANA-related peptide of 9-amino acids in length were found on the cell surface, while only 21 copies of the 10-amino acid form of this MANA were presented. Both the 9- and 10-amino acid forms were predicted to bind to HLA-A3 (predicted K_D of 1,172 and 939 nmol/L), respectively. Controls for these experiments included cells that were transfected with HLA but not the KRAS oncogene or vice versa, or cells transfected with HLA genes not expected to bind the MANA-related peptides. In all such cases, no peptides were detected by MANA-SRM.

Other MANA-related peptides that could be detected on the cell surface were those derived from KRAS mutations at codons 13 and 61, as well as IDH2 R140Q (Table 1). MANAs at Q61 were particularly well processed and presented, with up to 583 copies per cell. In contrast, mutations at the KRAS codon G12C, encoding MANAs that were predicted to bind to HLA-A3, were not detected by MANA-SRM. Because the identical procedures were used to evaluate each of these potential MANAs (transfection into COS-7 cells followed by MANA-SRM using the same antibody) and the heavy isotope-labeled G12C peptides were detected successfully, we conclude that the KRAS G12C peptides were processed inefficiently or that the *in silico* binding predictions were inaccurate.

Though not the primary purpose of MANA-SRM, this technique could also be used to assess endogenous processing and presentation of MANAs in cancer cells (rather than in transfected COS-7 cells). We found that Hs578.T lung cancer cells harboring an endogenous KRAS G12D mutation and an HLA-A3 genotype presented 71 copies of the G12D 9-mer by HLA per cell (Table 1). The G12D 10-mer, although also predicted to be present in these cells, was not detected. Controls for these experiments included IP with antibodies that did not bind to HLA but were of the same isotype. Additionally, only the abnormal peptides encoded by the mutant alleles present in these cells were detected by MANA-SRM. For example, G13D peptide–HLA complexes were not detected in cells harboring a G12D mutation, and vice versa.

Discussion

MANAs are critical inducers of T cell–mediated anticancer immune response (1, 24). Consequently, various immunotherapeutic approaches targeting defined MANAs have been developed (4, 8, 25–28). Given the efforts and time needed to develop the therapeutic agents against the target MANAs, it is imperative that the presentation on tumor cell surface of the predicted MANAs be verified before such efforts are initiated. Mass spectrometry analysis following IP with relevant anti-HLA antibodies represents a straightforward method to assess whether predicted MANAs are actually expressed, processed correctly, and presented by the HLA molecules (12). In practice, assessment of MANAs using this method has been challenging, especially when they are presented at low abundance and/or contain reactive amino acids susceptible to side-chain modifications such as cysteine and methionine (23).

We have developed an approach with several critical technical improvements that substantially increased the sensitivity of the published mass spectrometry methods used to identify MANAs. First, we systematically optimized protocols for cell lysis, IP, elution of peptides, as well as cross-linking of anti-HLA on beads to maximize yield of HLA–bound peptides while minimizing coelution of the antibody which otherwise could lead to signal suppression and reduced sensitivity of peptide detection. Second, we implemented a new streamlined procedure to purify the eluted peptides, which involved membrane filtration to remove HLA, followed by a hydrophobicity-based and a reverse phase HPLC-based chromatographic steps. Third, we identified derivatives from PEG commonly used in cell lysis and IP buffers as major contaminants and established an efficient method to remove

Published OnlineFirst September 16, 2019; DOI: 10.1158/2326-6066.CIR-19-0107

Table 1. Quantification of neoantigens through MANA-SRM

Cell line	Transfected	Endogenous HLA A alleles	Total # of cells (million)	Enriched by W6/32 antibody	Enriched by isotype control antibody	Predicted binding peptide by NetMHC 4.0	Predicted binding affinity by NetMHC 4.0 (unit: nmol/L, the lower value the stronger binding)	Detected abundance (femtomole)	Detected copy number per cell
COS-7	HLA-A3 + KRAS G12C vector	N/A	285.3	YES	NO	VVGACGVGK (9-mer)	221.43	N/D	N/D
		N/A				VVVGACGVGK (10-mer)	375.53	N/D	N/D
COS-7	HLA-A3 + KRAS G12D vector	N/A	270.9	YES	NO	VVGADGVGK (9-mer)	1,172.08	**64 ± 6.3**	**196 ± 19.3**
		N/A				VVVGADGVGK (10-mer)	938.8	**6 ± 0.53**	**21 ± 1.9**
COS-7	HLA-A3 + KRAS G13D vector	N/A	286.7	YES	NO	VVGAGDVGK (9-mer)	1,552.04	**26 ± 3.7**	**75 ± 10.7**
		N/A				VVVGAGDVGK (10-mer)	936.84	**2.2 ± 0.5**	**7 ± 1.6**
COS-7	HLA-A2 + KRAS G12C vector	N/A	261.9	YES	NO	N/A	N/A	N/D	N/D
COS-7	HLA-A2 + KRAS G12D vector	N/A	300.3	YES	NO	N/A	N/A	N/D	N/D
COS-7	HLA-A2 + KRAS G13D vector	N/A	276.6	YES	NO	N/A	N/A	N/D	N/D
COS-7	HLA-A1 + KRAS WT vector	N/A	290.2	YES	NO	ILDTAGQEEY	86.69	N/D	N/D
COS-7	HLA-A1 + KRAS Q61H vector	N/A	254.9	YES	NO	ILDTAGHEEY	185.91	**178 ± 12.2**	**583 ± 40.0**
COS-7	HLA-A2 + KRAS Q61H vector	N/A	266.2	YES	NO	N/A	N/A	N/D	N/D
COS-7	HLA-A1 + KRAS Q61L vector	N/A	267.6	YES	NO	ILDTAGLEEY	66.03	**136 ± 13.5**	**512 ± 50.8**
COS-7	HLA-A2 + KRAS Q61L vector	N/A	269.6	YES	NO	N/A	N/A	N/D	N/D
COS-7	HLA-A1 + KRAS Q61R vector	N/A	261.9	YES	NO	ILDTAGREEY	322.23	**40 ± 3.5**	**127 ± 11.1**
COS-7	HLA-B7 + IDH2 R140Q vector	N/A	273.3	YES	NO	SPNGTIQNIL	228.61	**8 ± 1.3**	**25 ± 4.1**
COS-7	HLA-B7 + IDH2 R140Q vector	N/A	289.2	NO	YES	N/A	N/A	N/D	N/D
COS-7	HLA-A3 + IDH2 R140Q vector	N/A	268.6	YES	NO	N/A	N/A	N/D	N/D
RPMI-6666	Not transfected	A*02:01, A*03:01	2,100	YES	NO	N/A	N/A	N/D	N/D
HH	Not transfected	A*01:01, A*01:01	2,000.0	YES	NO	N/A	N/A	N/D	N/D
CFPAC-1_G12D knock-in	Not transfected	A*02:01, A*03:01	83.1	YES	NO	VVGADGVGK (9-mer)	1,172.08	**4 ± 0.5**	**40 ± 5.0**
HS578.T	Not transfected	A*03:01, A*24:02	70.4	YES	NO	VVGADGVGK (9-mer)	1,172.08	**6 ± 0.6**	**71 ± 7.1**
HL-60	Not transfected	A*01:01, A*01:01	1,990.1	YES	NO	ILDTAGLEEY	66.03	**10 ± 1.0**	**4 ± 0.4**
SW948	Not transfected	A*01:01, A*01:01	326.1	YES	NO	ILDTAGLEEY	66.03	**6 ± 0.7**	**15 ± 1.75**
RD	Not transfected	A*01:01, A*01:01	412.9	YES	NO	ILDTAGHEEY	185.91	**4 ± 0.3**	**8 ± 0.6**
Hs940.T	Not transfected	A*01:01, A*01:01	131.3	YES	NO	ILDTAGREEY	322.23	**0.2 ± 0.02**	**1 ± 0.1**

Abbreviations: N/A, not available; N/D, not detectable.

them with the HILIC matrix. Fourth, we developed a dual-reduction strategy to prevent peptides containing methionine and/or cysteine from being modified, which improved the signals derived from these peptides by 300-fold. Together, the new approach with these improvements allowed us to detect endogenous MANAs with frequent driver mutations present at extraordinarily low abundance, likely in the single digit range as suggested by data shown in Table 1.

Massively parallel sequencing coupled with bioinformatics analyses routinely provides a list of candidate MANAs that could potentially be used in immunotherapy. MANA-SRM can determine, at unprecedented sensitivity, which of these candidate MANAs are actually processed and presented on the cell surface. The combination of these technologies thus paves the way for personalized and more effective immune-targeting therapies.

Published OnlineFirst September 16, 2019; DOI: 10.1158/2326-6066.CIR-19-0107

Disclosure of Potential Conflicts of Interest

Q. Wang is founder and CEO of and has ownership interest (including patents) in Complete Omics Inc. N. Papadopoulos is a shareholder, board of directors, at Thrive, is a shareholder/advisory board member at Personal Genome Diagnostics (PGDx) and NeoPhore, has ownership interest (including patents) in Thrive, PGDx, and NeoPhore, and is a consultant/advisory board member for Thrive, PGDx, and NeoPhore. K.W. Kinzler is an advisor for/founder of/member of the board of directors for Thrive, is a scientific advisor for Eisai-Morphotek and Sysmex-Inostics, is a consultant/advisory board member for NeoPhore, Phoremost, CAGE, and PGDx, and has ownership interest (including patents) in Thrive, NeoPhore, Phoremost, CAGE, and PGDx. S. Zhou reports receiving a commercial research grant from BioMed Valley Discoveries, has ownership interest (including patents) in Thrive, PGDx, and NeoPhore, and is a consultant/advisory board member for Guidepoint, PGDx, and NeoPhore. B. Vogelstein is founder of Thrive and PGDx, is an advisor for Sysmex, Eisai, CAGE, NeoPhore, and Nexus, and has ownership interest (including patents) in PGDx, Thrive, NeoPhore, and CAGE. No potential conflicts of interest were disclosed by the other authors.

Authors' Contributions

Conception and design: Q. Wang, J. Douglass, M. Zhang, K.W. Kinzler, S. Zhou, B. Vogelstein

Development of methodology: Q. Wang, J. Douglass, B. Vogelstein

Acquisition of data (provided animals, acquired and managed patients, provided facilities, etc.): Q. Wang, J. Douglass, M.S. Hwang, B.J. Mog, M. Zhang

Analysis and interpretation of data (e.g., statistical analysis, biostatistics, computational analysis): Q. Wang, J. Douglass, M.S. Hwang, E.H.-C. Hsiue, B.J. Mog, M. Zhang, N. Papadopoulos, K.W. Kinzler, S. Zhou

Writing, review, and/or revision of the manuscript: Q. Wang, J. Douglass, M.S. Hwang, B.J. Mog, N. Papadopoulos, K.W. Kinzler, S. Zhou, B. Vogelstein

Administrative, technical, or material support (i.e., reporting or organizing data, constructing databases): Q. Wang, J. Douglass, M.S. Hwang, B.J. Mog, M. Zhang

Study supervision: Q. Wang, N. Papadopoulos, K.W. Kinzler, S. Zhou, B. Vogelstein

Acknowledgments

The authors thank Srona Sengupta and Dr. Robert F. Siliciano for providing the CLIP DR*0101 and HIV Integrase DR1*0101 tetramers. The authors thank Agilent Technologies for providing some of the instrumentation pictures. This work was supported by the Lustgarten Foundation for Pancreatic Cancer Research, the Marcus Foundation, the Virginia and D.K. Ludwig Fund for Cancer Research, the Conrad R. Hilton Foundation, the Sol Goldman Center for Pancreatic Cancer Research, the Sol Goldman Sequencing Facility at Johns Hopkins, the Bloomberg Kimmel Institute at Johns Hopkins, and GI SPORE CA 62924, MSTP GM07309, and ONCOLOGY CORE CA 06973.

The costs of publication of this article were defrayed in part by the payment of page charges. This article must therefore be hereby marked *advertisement* in accordance with 18 U.S.C. Section 1734 solely to indicate this fact.

Received February 27, 2019; revised May 15, 2019; accepted September 4, 2019; published first September 16, 2019.

References

1. Schumacher TN, Schreiber RD. Neoantigens in cancer immunotherapy. Science 2015;348:69–74.
2. Riaz N, Morris L, Havel JJ, Makarov V, Desrichard A, Chan TA, et al. The role of neoantigens in response to immune checkpoint blockade. Int Immunol 2016;28:411–9.
3. Lauss M, et al. Mutational and putative neoantigen load predict clinical benefit of adoptive T cell therapy in melanoma. Nat Commun 2017;8:1738.
4. Ott PA, Hu Z, Keskin DB, Shukla SA, Sun J, Bozym DJ, et al. An immunogenic personal neoantigen vaccine for patients with melanoma. Nature 2017;547:217–221.
5. Diaz LA Jr, Le DT. PD-1 blockade in tumors with mismatch-repair deficiency. N Engl J Med 2015;373:1979.
6. Larkin J, Hodi FS, Wolchok JD. Combined nivolumab and ipilimumab or monotherapy in untreated melanoma. N Engl J Med 2015;373:1270–1.
7. Vitiello A, Zanetti M. Neoantigen prediction and the need for validation. Nat Biotechnol 2017;35:815–17.
8. Sahin U, Derhovanessian E, Miller M, Kloke BP, Simon P, Löwer M, et al. Personalized RNA mutanome vaccines mobilize poly-specific therapeutic immunity against cancer. Nature 2017;547:222–6.
9. The problem with neoantigen prediction. Nat Biotechnol 2017;35:97.
10. Lu YC, Yao X, Crystal JS, Li YF, El-Gamil M, Gross C, et al. Efficient identification of mutated cancer antigens recognized by T cells associated with durable tumor regressions. Clin Cancer Res 2014;20:3401–10.
11. Danilova L, Anagnostou V, Caushi JX, Sidhom JW, Guo H, Chan HY, et al. The mutation-associated neoantigen functional expansion of specific T cells (MANAFEST) assay: a sensitive platform for monitoring antitumor immunity. Cancer Immunol Res 2018;6:888–9.
12. Bassani-Sternberg M, Bräunlein E, Klar R, Engleitner T, Sinitcyn P, Audehm S, et al. Direct identification of clinically relevant neoepitopes presented on native human melanoma tissue by mass spectrometry. Nat Commun 2016;7:13404.
13. Creech AL, Ting YS, Goulding SP, Sauld JFK, Barthelme D, Rooney MS, et al. The role of mass spectrometry and proteogenomics in the advancement of HLA epitope prediction. Proteomics 2018;18:e1700259.
14. Hassan C, Kester MG, Oudgenoeg G, de Ru AH, Janssen GM, Drijfhout JW, et al. Accurate quantitation of MHC-bound peptides by application of isotopically labeled peptide MHC complexes. J Proteomics 2014;109:240–4.
15. Bassani-Sternberg M, Barnea E, Beer I, Avivi I, Katz T, Admon A, et al. Soluble plasma HLA peptidome as a potential source for cancer biomarkers. Proc Natl Acad Sci U S A 2010;107:18769–76.
16. Ternette N, Block PD, Sánchez-Bernabéu Á, Borthwick N, Pappalardo E, Abdul-Jawad S, et al. Early kinetics of the HLA class I-associated peptidome of MVA.HIVconsv-infected cells. J Virol 2015;89:5760–71.
17. Richardson CD, Ray GJ, DeWitt MA, Curie GL, Corn JE. Enhancing homology-directed genome editing by catalytically active and inactive CRISPR-Cas9 using asymmetric donor DNA. Nat Biotechnol 2016;34:339–44.
18. Agudelo D, Duringer A, Bozoyan L, Huard CC, Carter S, Loehr J, et al. Marker-free coselection for CRISPR-driven genome editing in human cells. Nat Methods 2017;14:615–20.
19. Wang Q, Zhang M, Tomita T, Vogelstein JT, Zhou S, Papadopoulos N, et al. Selected reaction monitoring approach for validating peptide biomarkers. Proc Natl Acad Sci U S A 2017;114:13519–24.
20. Andreatta M, Nielsen M. Gapped sequence alignment using artificial neural networks: application to the MHC class I system. Bioinformatics 2016;32:511–7.
21. Wang Q, Chaerkady R, Wu J, Hwang HJ, Papadopoulos N, Kopelovich L, et al. Mutant proteins as cancer-specific biomarkers. Proc Natl Acad Sci U S A 2011;108:2444–9.
22. Englard S, Seifter S. Precipitation techniques. Methods Enzymol 1990;182:285–300.
23. Lange V, Picotti Paola, Domon Bruno, Aebersold Ruedi. Selected reaction monitoring for quantitative proteomics: a tutorial. Mol Syst Biol 2008;4:222.
24. Yarchoan M, Hopkins A, Jaffee EM. Tumor mutational burden and response rate to PD-1 Inhibition. N Engl J Med 2017;377:2500–1.
25. Skora AD, Douglass J, Hwang MS, Tam AJ, Blosser RL, Gabelli SB, et al. Generation of MANAbodies specific to HLA-restricted epitopes encoded by somatically mutated genes. Proc Natl Acad Sci U S A 2015;112:9967–72.
26. Stronen E, Toebes M, Kelderman S, van Buuren MM, Yang W, van Rooij N, et al. Targeting of cancer neoantigens with donor-derived T cell receptor repertoires. Science 2016;352:1337–41.
27. Tran E, Robbins PF, Lu YC, Prickett TD, Gartner JJ, Jia L, et al. T-cell transfer therapy targeting mutant KRAS in cancer. N Engl J Med 2016;375:2255–62.
28. Tran E, Turcotte S, Gros A, Robbins PF, Lu YC, Dudley ME, et al. Cancer immunotherapy based on mutation-specific CD4+ T cells in a patient with epithelial cancer. Science 2014;344:641–5.

AACR American Association for Cancer Research

Cancer Immunology Research

Direct Detection and Quantification of Neoantigens

Qing Wang, Jacqueline Douglass, Michael S. Hwang, et al.

Cancer Immunol Res 2019;7:1748-1754. Published OnlineFirst September 16, 2019.